



Microwave ablation of *ex vivo* human undifferentiated pleomorphic sarcoma

Zhen-Jie Wu^{1*}, Wei-Hua Chen^{2*}, Ju-Liang He¹, Bin Liu¹, Hao Mo¹, Jian Guan¹, Xiang Lin¹, Zhen-Chao Yuan¹

¹Department of Bone and Soft Tissue Surgery, Affiliated Tumor Hospital of Guangxi Medical University, Nanning 530021, China; ²Department of Children Rehabilitation, Maternal and Child Health Hospital of Guangxi Zhuang Autonomous Region, Nanning 530003, China

Contributions: (I) Conception and design: ZJ Wu, ZC Yuan; (II) Administrative support: WH Chen; (III) Provision of study materials or patients: JL He, B Liu, H Mo; (IV) Collection and assembly of data: JL He, J Guan, X Lin; (V) Data analysis and interpretation: ZJ Wu, WH Chen, B Liu; (VI) Manuscript writing: All authors; (VII) Final approval of manuscript: All authors.

*These authors contributed equally to this work.

Correspondence to: Zhen-Chao Yuan. He Di Rd. #71, Nanning 530021, China. Email: yuanchenchao126@126.com.

Background: Many undifferentiated pleomorphic sarcoma (UPS) patients had lost the opportunity of surgical therapy. Microwave (MW) ablation of UPS can be an effective method for achieving local tumor control while preserving the relative function. We report for the first time the size of the ablation zone and temperature distribution of MW ablation on *ex vivo* human UPS specimens.

Methods: Twenty UPS patients' specimens were recruited into present experimental study (11 men, 9 women, average age 52 ± 14.7 years). A commercial 2,450 MHz MW ablation apparatus was used throughout this experiment. MW ablations were performed immediately after resection of tissue specimens by using powers of 40, 60, 80 and 100 W for 10 min, and each power setting was performed in five specimens. Coagulation shape, lesion size, and temperature distributions were recorded. Histological examination was performed to assess the pathological changes of the ablation issue.

Results: All coagulation geometries were ellipsoidal under the four power settings (40, 60, 80 and 100 W for 10 min) with a ratio of short-axis/long-axis range from 0.80 to 0.88. The short-axis diameters of the coagulation at 40, 60, 80 and 100 W groups were 28.2 ± 1.1 , 35.6 ± 1.3 , 40.6 ± 1.6 , and 46.4 ± 1.7 mm, respectively; and the corresponding long-axis were 33.4 ± 1.5 , 41.4 ± 1.7 , 47.6 ± 1.8 , and 54.2 ± 2.1 mm, respectively. Overall, temperatures at 3 points of distance 10, 20, and 30 mm from antenna increased along with ablation time. Routine histological analysis using haematoxylin-eosin (H&E) showed tissue fixation within the ablation area.

Conclusions: The present *ex vivo* experiment showed that MW ablation by single 2,450 MHz antennae could generate an ellipsoidal coagulation geometry and large ablation zone, which increases with increasing power and time. This initial study provides experimental evidence for clinical MW ablation of UPS.

Keywords: Microwave ablation (MW ablation); *ex vivo* experiment; undifferentiated pleomorphic sarcoma (UPS)

Submitted Sep 30, 2017. Accepted for publication Feb 26, 2018.

doi: 10.21037/tcr.2018.03.01

View this article at: <http://dx.doi.org/10.21037/tcr.2018.03.01>

Introduction

Soft tissue sarcomas (STS) are a heterogeneous group of rare malignant neoplasms arising from mesodermal tissues. STS account for approximately 1% of all adult malignancies (1). Malignant fibrous histiocytoma (MFH) is a common

histological subtype of STS in adults, which is first reported in 1961 as a histiocytic tumor with storiform growth (2) and now is reclassified as "high-grade undifferentiated pleomorphic sarcoma (UPS)" by the World Health Organization in 2002.

The mainstay of treatment for UPS is margin-negative

surgical resection adding radiotherapy or chemotherapy if necessary (3). However, about 13–42% of patients suffer a local recurrence following aggressive surgery and nearly one-third develop metastatic disease (4). Although there is no standard treatment for local recurrences, minimization of the STS in the body is advocated to improve the long-term survival rates (5,6). Therefore, it is important to explore a safe and effective method for patients who are suffering recurrent STS and are no longer surgical candidates.

In recent years, imaging-guided thermal ablation for local tumors—including radiofrequency, microwave (MW), cryoablation, laser, etc.—has been a great development due to modern technological progress (7–9). Particularly, MW ablation, denaturing the protein instantaneously by utilizing the very high temperature increase, is being increasingly used for local tumors such as liver, lung, and kidney, because of its minimal invasiveness and larger coagulation volumes (10–12).

However, few publications in the English language literature specifically evaluate the clinical utility of MW ablation in controlling recurrent STS (13) or its impact on patient prognosis, especially in UPS. Moreover, so far, there is no relevant preclinical data (such as *ex vivo*, *in vivo*, animal model, etc.) for clinicians' reference, such as the MW ablation zone and distribution in UPS.

In fact, many UPS patients had lost the opportunity of surgical therapy including the elderly, who cannot tolerate surgery, those who have postoperative recidivation which had struck a major blood vessel and/or nerve, and those who have retroperitoneal huge tumor without nonspecific symptoms at early stage. We hypothesize that MW ablation of UPS can be an effective method for achieving local tumor control while preserving the relative function.

The purpose of this initial study is to report the size of the ablation zone and temperature distribution of MW ablation on *ex vivo* human UPS specimen.

Methods

Patients and specimens

The present study included patients suffering UPS who received regular treatment with their *ex vivo* specimens being used as experimentations. Twenty UPS patients were recruited into present experimental study (11 men, 9 women, average age 52 ± 14.7 years) (Table 1). Guangxi Medical University Ethics Committee gave ethical approval for the present study, and all the included patients provided

written informed consent for their tissues to be used in this study. All the patients received radical resection, and no patients receive any chemotherapy or radiotherapy treatment prior to resection. Once the specimen is delivered from the patient undergoing surgery, MW ablations were performed immediately (typical time to first ablation <120 s). The minimum diameter of all specimens included was greater than 5 cm. One ablation was performed on each individual *ex vivo* specimen.

MW system

A MW delivery system (ECO-100CI9, ECO Medical, Nanjing, China) was selected in the present experiment. This system consisted of a MW generator with frequencies of 2,450 MHz, a power output of 10–120 W, a flexible low-loss cable, a water-pumping machine, and a 14-gauge cooled-shaft antenna. The cooled-shaft antenna contained a 20 cm shaft coated with Teflon with a diameter of 2.0 mm, a narrow radiating segment of 1.5 mm embedded on the shaft, and a 1.5-cm-long active tip. The antenna has two lumina to deliver cooled water to the tip of the shaft and return the warmed water to a 500 mL plastic bag. The system also contained a steady flow pump pushing the cooled water in the antenna shaft passage at a rate of 20 mL/min to maintain the shaft at a relatively low temperature during ablation.

Ablation protocol

Ablations were performed in *ex vivo* human UPS using powers of 40, 60, 80 and 100 W at 2,450 MHz with ablating time of 10 min at environmental temperature (29 ± 2 °C), and each power setting was performed in five specimens. The cooled-shaft antenna was inserted 5 cm into the tumor specimen to ensure that the whole ablation area would be within the tumor. Temperature was measured along the short axis of the ablation zone by using three 18-gauge thermistor probes (response time 55 s, accuracy 0.1 °C), which were parallelly placed at points of distance 10 (t1), 20 (t2), and 30 mm (t3) from antenna. Temperatures were recorded at 5-second intervals for each ablation. After ablation, the resected specimen was dissected along the needle track to show the thermal lesion (Figure 1), and two assessors (Ju-Liang He and Jian Guan) measured the maximal cross-sectional length (the long-axis diameter) and width (the short-axis diameter) of the ablation zone using calipers. We also calculate the ratio of short/long axis to

Table 1 Patient information and coagulation necrosis parameters of MW ablation

Patients	Age (year)	Sex	Size of tumor (mm ³)	Power, duration	Long-axis (mm)	Short-axis (mm)	Ratio	T1 (°C)	T2 (°C)	T3 (°C)
1	55	F	75×60×60	40 W, 10 min	32	28	0.88	106.9	61.5	44.5
2	40	M	79×62×68	40 W, 10 min	33	27	0.81	107.1	60.8	43.5
3	47	M	82×70×66	40 W, 10 min	35	29	0.83	105.2	60.7	43.8
4	59	F	85×71×68	40 W, 10 min	34	30	0.88	106.5	62.7	44.8
5	49	F	95×85×72	40 W, 10 min	33	27	0.82	108.2	63.7	45.2
6	35	M	99×88×70	60 W, 10 min	41	36	0.88	118.2	66.8	45.9
7	70	F	123×100×95	60 W, 10 min	40	35	0.88	117.5	65.9	46.8
8	48	M	125×110×86	60 W, 10 min	43	37	0.86	117.9	67.5	45.7
9	59	M	145×110×90	60 W, 10 min	41	36	0.88	119	67.8	45.9
10	57	F	155×120×92	60 W, 10 min	42	34	0.81	116.5	69.5	45.1
11	37	M	160×102×95	80 W, 10 min	45	39	0.86	125.7	75.8	47.2
12	55	F	168×109×99	80 W, 10 min	47	40	0.85	123.9	76.1	48.5
13	58	F	165×116×75	80 W, 10 min	48	41	0.85	124.8	75.8	49.5
14	71	M	175×126×76	80 W, 10 min	49	42	0.86	126.7	77.9	49.5
15	36	M	185×90×88	80 W, 10 min	49	41	0.84	123.8	78.9	48.6
16	39	F	195×100×99	100 W, 10 min	52	46	0.88	131.8	88.5	57.9
17	79	M	192×117×90	100 W, 10 min	53	48	0.87	134.9	86.9	56.7
18	48	F	205×137×100	100 W, 10 min	55	45	0.8	135.9	89.5	59.2
19	45	M	210×140×125	100 W, 10 min	54	47	0.85	130.4	87.5	58.4
20	60	M	280×160×135	100 W, 10 min	57	46	0.81	132.8	90	57.8

MW, microwave; F, female; M, male; ratio, the ratio of short-axis/long-axis; T1, T2, T3 indicated that the highest temperature (°C) at location t1, t2, t3.

simply describe the sphericity index of the ablation zone. The ablated area contained two visually obvious zones, the center zone (charring zone) and the gray zone (coagulation zone).

Histological analysis

Multiple sections of ablated and untreated UPS were sampled for haematoxylin-eosin (H&E) pathological analysis. Immediately after sampling, they were placed in sampling cassettes and immersed in formalin. The pathology results were reviewed by the same pathologist.

Statistical analysis

Results of lesion diameters and temperature data were given as mean ± standard deviation (SD). Differences in the long-

axis diameter, short-axis diameter, and temperatures between groups were evaluated by independent samples *t*-test. Data were analyzed with use of Stata software (version 11.0; Stata Corporation, College Station, TX, USA). P value less than 0.05 was considered statistically significant.

Results

Coagulation shape and lesion size

All coagulation geometries were ellipsoidal under the four power settings (40, 60, 80 and 100 W for 10 min) with a ratio of short-axis/long-axis range from 0.80 to 0.88. An arrow-shaped charring around the axis was detected in each group. As the power output increased, all MW ablation areas showed a trend of increase. The short-axis diameters

of the coagulation at 40, 60, 80 and 100 W groups were 28.2 ± 1.1 , 35.6 ± 1.3 , 40.6 ± 1.6 , and 46.4 ± 1.7 mm, respectively; and the corresponding long-axis were 33.4 ± 1.5 , 41.4 ± 1.7 , 47.6 ± 1.8 , and 54.2 ± 2.1 mm, respectively.

Temperature distributions

We collected the data of temperature variation at t1, t2

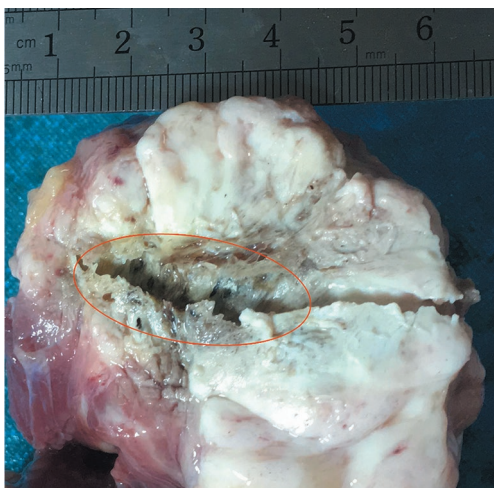


Figure 1 Ablated region of microwave ablation. Ellipsoidal ablated region of microwave ablation by using the 2,450 MHz antenna at 40 W for 10 minutes in *ex vivo* human UPS specimen. The ellipsoidal gray area (red circle) is coagulation zone. The charring is arrow-shaped. UPS, undifferentiated pleomorphic sarcoma.

and t3 location under different ablation conditions. The time-temperature curves are shown in *Figure 2*. Overall, experiments showed that temperatures of t1, t2, and t3 increased along with ablation time. For t1 and t2, higher power in MW ablation tended to generate higher temperatures, which can eventually exceed 60 °C. For t3 (except for 100 W), different ablation powers eventually yield a similar temperature at the end of the procedure (about 47 °C), and temperature of t3 for 100 W eventually reached 60 °C.

Histological analysis

Morphological change of cells was observed by H&E staining. Tumor cells before ablation (*Figure 3A*) showed diffuse distribution or nest the bands of arrangement with clear cytoplasm. After ablation (*Figure 3B*), the outline of the cancer cells was ambiguous with red staining cytoplasm, and nucleus dissolved and shrunk.

Discussions

In recent years, the application of MW ablation on primary and metastatic solid malignant tumor has received more and more attention because of its effectiveness, safety, analgesic potential, and practicability (14,15). Effects of heat of MW ablation cause irreversible cellular destruction at temperatures above 50 °C for about 5 min and almost immediately at temperatures above 60 °C (16). To the best

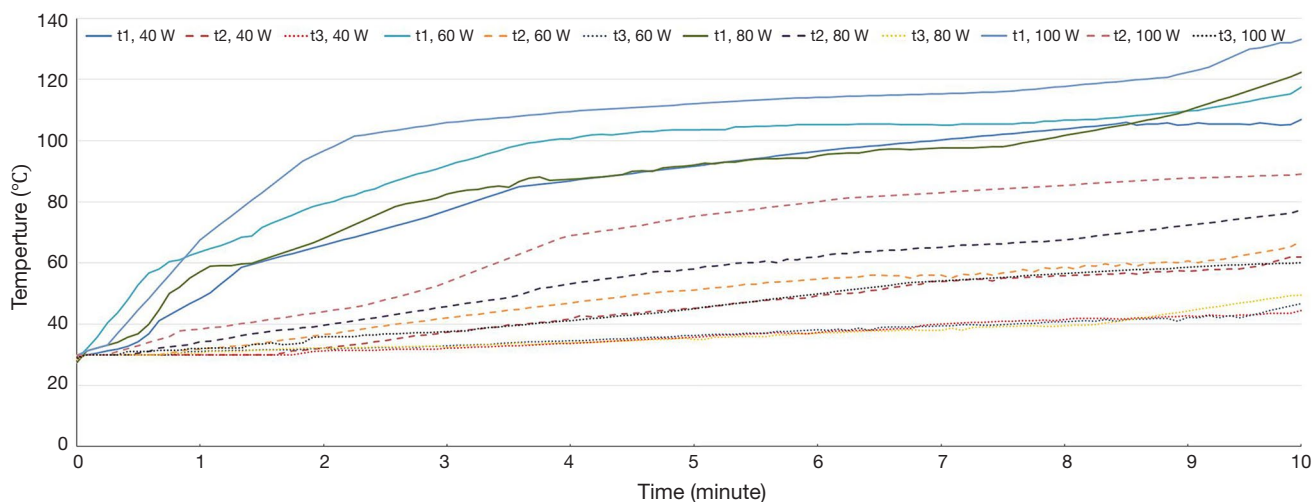


Figure 2 Time-temperature curves. Temperature at points of distance 10 mm (t1, solid line), 20 mm (t2, long dashed line), and 30 mm (t3, short dashed line) from the antenna at 40, 60, 80, and 100 W for 10 minutes.

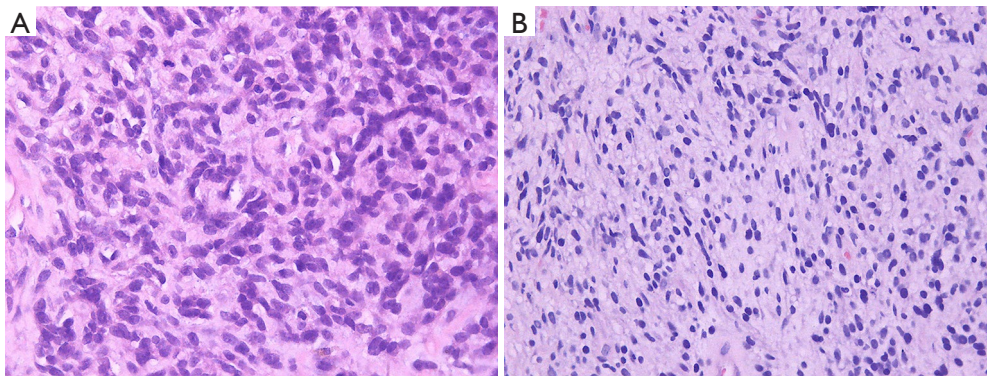


Figure 3 Untreated (A) and ablated (B) UPS specimen $\times 400$ (H&E stain). Untreated tumor cells showed diffuse distribution or nest the bands of arrangement with clear cytoplasm. After ablation, the outline of the cancer cells was ambiguous with red staining cytoplasm, and nucleus dissolved and shrunken. UPS, undifferentiated pleomorphic sarcoma.

of our knowledge, the coagulation shape and temperature distribution of MW ablation for the treatment of STS has never been evaluated by using *ex vivo* human specimens. Only a few clinical studies (13,14) with small sample sizes of STS have been conducted, showing promising results. The present experiment, for the first time, demonstrated that a 2,450 MHz and 2.0 mm diameter antennae can develop ellipsoid zones (the ratio of short-axis/long-axis ranged from 0.80 to 0.88) of ablation with the maximum of short-axis coagulation diameter of 46.4 mm (100 W for 10 min) in *ex vivo* human UPS specimens.

The ideal thermal ablation should be to design an optimal ablation protocol based on known ablation shape and temperature distributions that will allow seamless ablation and protection of the major nerves and blood vessels around the tumor. Usually, if the complete ablation is acquired, tumor may be controllable. But, if incomplete ablation, tumor may be increasing soon. The ability of precisely predicting the ablation shape and temperature distributions when making an ablation plan can decide whether the thermal ablation treatment will be successful or not (17-19).

We chose 40, 60, 80, and 100 W for 10 min as ideal power settings in present initial experiment. All coagulation geometries were ellipsoidal with a ratio of short-axis/long-axis range from 0.80 to 0.88. As the number of MW ablation power output increased, the maximum of short-axis coagulation diameter had gradually increased and reached the maximum at the power setting of 100 W for 10 min. The temperatures of t_1 , t_2 , and t_3 increased along with ablation time. Our results were similar with a recent study (20), which reported that ablation diameter was

37 ± 3 mm at 60 W for 10 min for *ex vivo* human hepatocellular carcinomas specimen, with an average sphericity index of 0.70 ± 0.04 . However, the sphericity index in present study were less than those using a pair of internally interstitial MW applicators, which were almost all >0.85 for *ex vivo* porcine livers (21).

MW ablation can result in tissue fixation within the ablation area (22). The pathological histology analysis of ablated tissue from this study showed the same effect.

One of the advantages of the present study is that we conducted the experiment directly with the fresh *ex vivo* human UPS specimens, and the results would be of great significance to the clinic application. We found that, even for the specimen of the same UPS patient, there are slightly differences in homogeneity, density, and thermophysical properties of tumor tissue, which would result in different coagulation zone and temperature distribution for the same ablation power output and time. While some reports (23) used fresh bovine liver as the proxy for human liver tumors, which were high differences in homogeneity, density of tumor tissue, the experimental results were more different from clinical applications.

There are several limitations to present study. Firstly, our experiments were conducted on *ex vivo* UPS specimen tissue thus, like any similar research, underestimating the impact of blood perfusion. Secondly, our experiments were performed with a limited number of specimens and cannot be able to further study the relevant issues. To reduce experimental error, all the selected UPS patients were confirmed by puncture pathology, and did not received any chemotherapy and/or radiotherapy before operation, and had the specimen more than 5 cm in the minimum diameter.

Moreover, with the low incidence of UPS, it is not easy to collect enough specimens and then perform experiments. Further studies are needed to confirm these findings and carry out in-depth research, both increasing the number of specimens and *in vivo* animal model studies. Finally, we used only one probe in MW ablation process. Using two probes simultaneously may generate more spherical coagulation zones and improve the efficiency of ablation. Shi *et al.* (23) reported that simultaneous application of double antennae can achieve larger ablations which can cover the entire tumor region in one ablation session.

In conclusion, the present *ex vivo* experiments showed that MW ablation by single 2,450 MHz antennae could generate an ellipsoidal coagulation geometry and large ablation zone, which increases with increasing power and time. This study provides experimental evidence for clinical MW ablation of UPS.

Acknowledgments

Funding: This work was supported by Youth Science Foundation of Guangxi Medical University (GXMUYSF201331), and Open Project of Guangxi Key Laboratory of Biological Targeting Diagnosis and Therapy Research (2015-04).

Footnote

Conflicts of Interest: All authors have completed the ICMJE uniform disclosure form (available at <http://dx.doi.org/10.21037/tcr.2018.03.01>). The authors have no conflicts of interest to declare.

Ethical Statement: The authors are accountable for all aspects of the work in ensuring that questions related to the accuracy or integrity of any part of the work are appropriately investigated and resolved. The study was conducted in accordance with the Declaration of Helsinki (as revised in 2013). Guangxi Medical University Ethics Committee gave ethical approval for the present study (No. 2017-098). All the included patients provided written informed consent for their tissues to be used in this study.

Open Access Statement: This is an Open Access article distributed in accordance with the Creative Commons Attribution-NonCommercial-NoDerivs 4.0 International License (CC BY-NC-ND 4.0), which permits the non-commercial replication and distribution of the article with the strict proviso that no changes or edits are made and the

original work is properly cited (including links to both the formal publication through the relevant DOI and the license). See: <https://creativecommons.org/licenses/by-nc-nd/4.0/>.

References

1. Singer S, Demetri GD, Baldini EH, et al. Management of soft-tissue sarcomas: an overview and update. *Lancet Oncol* 2000;1:75-85.
2. Kauffman SL, Stout AP. Histiocytic tumors (fibrous xanthoma and histiocytoma) in children. *Cancer* 1961;14:469-82.
3. Belal A, Kandil A, Allam A, et al. Malignant fibrous histiocytoma: a retrospective study of 109 cases. *Am J Clin Oncol* 2002;25:16-22.
4. Delisca GO, Mesko NW, Alamanda VK, et al. MFH and high-grade undifferentiated pleomorphic sarcoma-what's in a name? *J Surg Oncol* 2015;111:173-7.
5. Zer A, Prince RM, Amir E, et al. Evolution of Randomized Trials in Advanced/Metastatic Soft Tissue Sarcoma: End Point Selection, Surrogacy, and Quality of Reporting. *J Clin Oncol* 2016;34:1469-75.
6. Qu X, Lubitz CC, Rickard J, et al. A Meta-Analysis of the Association Between Radiation Therapy and Survival for Surgically Resected Soft-Tissue Sarcoma. *Am J Clin Oncol* 2018;41:348-56.
7. Meloni MF, Chiang J, Laeseke PF, et al. Microwave ablation in primary and secondary liver tumours: technical and clinical approaches. *Int J Hyperthermia* 2017;33:15-24.
8. Jiao D, Qian L, Zhang Y, et al. Microwave ablation treatment of liver cancer with 2,450-MHz cooled-shaft antenna: an experimental and clinical study. *J Cancer Res Clin Oncol* 2010;136:1507-16.
9. Cazzato RL, Garnon J, Ramamurthy N, et al. Percutaneous image-guided cryoablation: current applications and results in the oncologic field. *Med Oncol* 2016;33:140.
10. Lin Y, Liang P, Yu XL, et al. Percutaneous microwave ablation of renal cell carcinoma is safe in patients with renal dysfunction. *Int J Hyperthermia* 2016:1-6.
11. Biederman DM, Titano JJ, Bishay VL, et al. Radiation Segmentectomy versus TACE Combined with Microwave Ablation for Unresectable Solitary Hepatocellular Carcinoma Up to 3 cm: A Propensity Score Matching Study. *Radiology* 2017;283:895-905.
12. Ni Y, Ye X, Wan C, et al. Percutaneous microwave ablation (MWA) increased the serum levels of VEGF and MMP-9 in Stage I non-small cell lung cancer (NSCLC).

- Int J Hyperthermia 2017;1-5.
13. Aubry S, Dubut J, Nueffer JP, et al. Prospective 1-year follow-up pilot study of CT-guided microwave ablation in the treatment of bone and soft-tissue malignant tumours. *Eur Radiol* 2017;27:1477-85.
 14. Kastler A, Alnassan H, Pereira PL, et al. Analgesic effects of microwave ablation of bone and soft tissue tumors under local anesthesia. *Pain Med* 2013;14:1873-81.
 15. Ma S, Ding M, Li J, et al. Ultrasound-guided percutaneous microwave ablation for hepatocellular carcinoma: clinical outcomes and prognostic factors. *J Cancer Res Clin Oncol* 2017;143:131-42.
 16. Goldberg SN, Gazelle GS, Mueller PR. Thermal ablation therapy for focal malignancy: a unified approach to underlying principles, techniques, and diagnostic imaging guidance. *AJR Am J Roentgenol* 2000;174:323-31.
 17. Cavagnaro M, Amabile C, Cassarino S, et al. Influence of the target tissue size on the shape of ex vivo microwave ablation zones. *Int J Hyperthermia* 2015;31:48-57.
 18. Ryan TP, Brace CL. Interstitial microwave treatment for cancer: historical basis and current techniques in antenna design and performance. *Int J Hyperthermia* 2017;33:3-14.
 19. Lopresto V, Pinto R, Farina L, et al. Treatment planning in microwave thermal ablation: clinical gaps and recent research advances. *Int J Hyperthermia* 2017;33:83-100.
 20. Amabile C, Ahmed M, Solbiati L, et al. Microwave ablation of primary and secondary liver tumours: ex vivo, in vivo, and clinical characterisation. *Int J Hyperthermia* 2017;33:34-42.
 21. Li X, Zhang L, Fan W, et al. Comparison of microwave ablation and multipolar radiofrequency ablation, both using a pair of internally cooled interstitial applicators: results in ex vivo porcine livers. *Int J Hyperthermia* 2011;27:240-8.
 22. Bhardwaj N, Strickland AD, Ahmad F, et al. A comparative histological evaluation of the ablations produced by microwave, cryotherapy and radiofrequency in the liver. *Pathology* 2009;41:168-72.
 23. Shi W, Liang P, Zhu Q, et al. Microwave ablation: results with double 915 MHz antennae in ex vivo bovine livers. *Eur J Radiol* 2011;79:214-7.

Cite this article as: Wu ZJ, Chen WH, He JL, Liu B, Mo H, Guan J, Lin X, Yuan ZC. Microwave ablation of *ex vivo* human undifferentiated pleomorphic sarcoma. *Transl Cancer Res* 2018;7(2):283-289. doi: 10.21037/tcr.2018.03.01